J. Fluid Mech. (1977), *vol.* 81, *part* 2, *pp.* 265–272
Printed in Great Britain

Novel Weissenberg effects

By G. S. BEAVERS AND D. D. JOSEPH
Department of Aerospace Engineering and Mechanics,
University of Minnesota, Minneapolis

(Received 30 June 1976 and in revised form 5 January 1977)

We have observed two novel manifestations of the Weissenberg effect in viscoelastic liquids which are set into motion by the rotation of a circular rod. In the first experiment we floated a layer of STP on water. The STP climbs up the rod into the air and down the rod into the water. The 'down-climb' is much larger than the 'up-climb', their ratio being roughly the square root of the density difference (STP–air)/(water–STP). The magnification of the down-climb may be regarded as *normal-stress amplification*.† The magnitudes of the up- and down-climbs are simultaneously in good agreement with the predictions of a theory of rod climbing when the angular frequency of the rod is small. In the second experiment, we set the rod into torsional oscillations. When the amplitude of the oscillation is small, the fluid climbs the rod; the climb is divided into an axisymmetric steady mean part and an oscillating part (Joseph 1976*b*; Beavers 1976). The mean axisymmetric climb dominates the total climb at low frequencies. At a higher critical speed the axisymmetric climbing bubble loses its stability to another time-periodic motion with the same period but with a 'flower' pattern displaying a certain integral number of petals.

1. A normal-stress amplifier: the free surfaces on a viscoelastic liquid floating on water

We shall first give a brief analysis which shows that when the angular frequency Ω of the rod is small the height rise at each interface is decoupled and can be obtained from formulae similar to those given by Joseph, Beavers & Fosdick (1973) and Beavers & Joseph (1975). In comparing the analysis of the three-fluid configuration given here with the earlier analyses three points of difference deserve emphasis.

(i) In this analysis we solve the dynamical problem as a coupled problem in all three layers. Correct coupling conditions for continuity of stresses at each of the two inter-

† The idea of using a second fluid as a' normal-stress amplifier' could be inferred from incidental remarks in the report by Saville & Thompson (1969) on experiments on secondary flows associated with the Weissenberg effect. They used two guard fluids of about equal density to suppress the effects of the ends on the secondary flows. They concluded their report on secondary flows with the observation that: "Further experiments indicated that the motion was downward along the shaft in the upper main toroidal eddy and upward along the shaft in the upper bead. At the lower interface of the non-Newtonian liquid, normal stresses have caused downward extrusion of this liquid, quite similar to the more familiar rod climbing exhibited in the upper bead. Choosing 'guard' liquids with densities near that of the non-Newtonian liquid increases the size of the beads thus accentuating the effects of normal stresses. The existence of such a secondary flow emphasizes the complex nature of flows of non-Newtonian fluids and the usefulness of flow visualization techniques."

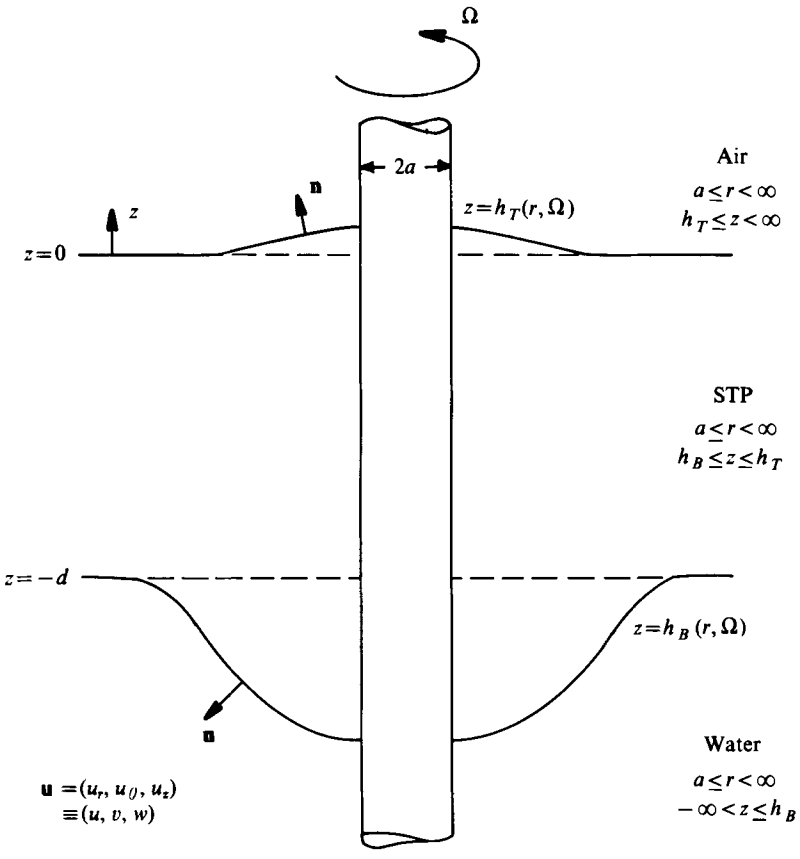

FIGURE 1. Schematic sketch of the free surfaces on STP floating on water.

faces are prescribed. For example, we require the tangential tractions to be continuous across each interface and we do not assume that the tangential tractions of air and water on STP are negligible. Despite this, the analysis shows that no secondary motion is generated at second order in Ω where the deviation from a flat free surface first occurs.

(ii) The shape of the STP–air interface is the same as that given by equation (16.2) of Joseph *et al.* (1973) or by equation (6.5) of Beavers & Joseph (1975) if the density ρ of STP is replaced by $\rho - \rho_a$ ($\approx \rho$), where ρ_a is the density of air.

(iii) The shape of the water–STP interface also depends on a density difference, $\rho_w - \rho$, where ρ_w is the density of water, but the shape of the free surface is not similar to that of the STP–air surface. The effect of inertia and gravity is to push the heavy fluid down near the rod. The normal stresses push the STP up into the air and down into the water. Hence inertia and normal stresses are in conflict at the STP–air interface and in concert at the water–STP interface.

The configuration under discussion is sketched in figure 1. The basic analysis for the shape of the free surface has been given in Joseph *et al.* (1973) and Beavers & Joseph (1975), hereafter designated as I and II respectively. We shall now show how the formulae for the free surface given in I and II may be adapted to give the shapes of the free surfaces $z = h_T(r, \Omega)$ and $z = h_B(r, \Omega)$ depicted in figure 1.

We shall assume that the motions are isochoric and that the fluid satisfies the no-slip condition at the rod surface. Then $\operatorname{div}\mathbf{u} = 0$ and $\mathbf{u}(a, z, \Omega) = \mathbf{e}_\theta a\Omega$ simultaneously in the air, STP and water. Apart from the hydrostatic pressure, all other flow variables are to be independent of z as $\pm z \to \infty$.

The dynamic equations are

$$\rho_a \mathbf{u}.\nabla\mathbf{u} = -\nabla\Phi_a + \mu_a\nabla^2\mathbf{u} \quad \text{(air)}, \tag{1}$$

$$\rho\mathbf{u}.\nabla\mathbf{u} = -\nabla\Phi + \nabla.\mathbf{S} \quad \text{(STP)}, \tag{2}$$

$$\rho_w \mathbf{u}.\nabla\mathbf{u} = -\nabla\Phi_w + \mu_w\nabla^2\mathbf{u} \quad \text{(water)}. \tag{3}$$

Here $\mathbf{S}$ is the extra stress, $\Phi = p + \rho gz$ is the head, p is the pressure of constraint, and (ρ_a, μ_a, Φ_a), (ρ_w, μ_w, Φ_w) and (ρ, μ, Φ) are the (density, viscosity, head) of air, water and STP.

The interface conditions are as follows (see I, p. 327).

(i) No fluid crosses an interface; the normal component $\mathbf{u}.\mathbf{n}$ of velocity is zero at an interface. In co-ordinate form the vanishing of the normal component of velocity may be expressed as

$$w = h'u \quad \text{on} \quad z = h_T, h_B. \tag{4}$$

(ii) The shear tractions in co-ordinate form,

$$S_{z\theta} - h'S_{r\theta} \tag{5}$$

and

$$h'(S_{zz} - S_{rr}) + (1 - h'^2)S_{rz}, \tag{6}$$

are continuous across the interfaces $z = h_B$ and $z = h_T$.

(iii) The jump in the normal component of the stress is balanced by surface tension:

$$\begin{aligned} 0 &= (-p + S_{nn}) - (-p_a + 2\mu_a D^{(a)}_{nn}) - T_T r^{-1}[rh'_T/(1+h'^2_T)^{\frac{1}{2}}]' \\ &= -\Phi + \Phi_a + S_{nn} - 2\mu_a D^{(a)}_{nn} + (\rho - \rho_a)gh_T - T_T r^{-1}[rh'_T/(1+h'^2_T)^{\frac{1}{2}}]' \end{aligned} \tag{7}$$

on $z = h_T$ and, in a similar way,

$$0 = -\Phi + \Phi_w + S_{nn} - 2\mu_w D^{(w)}_{nn} + (\rho - \rho_w)gh_B + T_B r^{-1}[rh'_B/(1+h'^2_B)^{\frac{1}{2}}]' \tag{8}$$

on $z = h_B$, where $S_{nn} = \mathbf{n}.\mathbf{S}.\mathbf{n}$ and $D_{nn} = \mathbf{n}.\mathbf{D}.\mathbf{n}$ are the normal components of the extra stress and rate-of-strain tensors, respectively, and T_T and T_B are the surface-tension coefficients at the top and bottom interfaces. In co-ordinate form

$$S_{nn} = (S_{zz} + S_{rr}h'^2 - 2h'S_{zr})/(1+h'^2). \tag{9}$$

(iv) Asymptotically as $r \to \infty$ the free surface is flat and the distance between h_B and h_T is d. We choose $z = 0$ such that

$$\left.\begin{aligned} h_T(\infty, \Omega) &= 0; \\ h_B(\infty, \Omega) &= -d. \end{aligned}\right\} \tag{10}$$

then

(v) The perturbation analysis of I requires that the contact conditions at $r = a$ are compatible with a flat free surface in the rest state. These are taken as

$$h'_T(a, \Omega) = h'_B(a, \Omega) = 0. \tag{11}$$

The solution of the problem (1)–(11) may be constructed as a perturbation of the rest state in powers of Ω. The azimuthal components of the velocity and shear stress are

odd functions of Ω while the shape of the free surface, the pressure, the secondary motion and the normal stress are even functions of Ω. The extra stress $\mathbf{S}$ is expanded into a series of Rivlin–Ericksen tensors in the usual way (see I, II). We shall outline the analysis up to order two.

When $\Omega = 0$, $\mathbf{u} = \mathbf{u}^{\langle 0\rangle} = 0$, $\Phi = \Phi^{\langle 0\rangle} = 0$, $h_T = h_T^{\langle 0\rangle} = 0$ and $h_B = h_B^{\langle 0\rangle} = -d$. At first order all conditions are satisfied with

$$\mathbf{u}^{\langle 1\rangle} = [\partial \mathbf{u}(r, z, \Omega)/\partial\Omega]_{\Omega=0} = \mathbf{e}_\theta a^2/r^2. \tag{12}$$

Of course, $h^{\langle 1\rangle}$ and $\Phi^{\langle 1\rangle}$ vanish identically.

Proceeding as on page 485 of II, we find that at order two (1)–(3) become

$$\mathbf{e}_r \frac{d}{dr}\left[\frac{\rho_a a^4}{2r^2}\right] = -\nabla\Phi_a^{\langle 2\rangle} + \mu_a \nabla^2 \mathbf{u}^{\langle 2\rangle}, \tag{13}$$

$$-\mathbf{e}_r \frac{d}{dr}\left[\frac{2a^4\hat{\beta}}{r^4} - \frac{\rho a^4}{2r^2}\right] = -\nabla\Phi^{\langle 2\rangle} + \mu \nabla^2 \mathbf{u}^{\langle 2\rangle}, \tag{14}$$

where $\hat{\beta} = 3\alpha_1 + 2\alpha_2$ is the climbing constant, and

$$\mathbf{e}_r \frac{d}{dr}\left[\frac{\rho_w a^4}{2r^2}\right] = -\nabla\Phi_w^{\langle 2\rangle} + \mu_w \nabla^2 \mathbf{u}^{\langle 2\rangle}. \tag{15}$$

The inhomogeneous terms in (13)–(15) are of potential type and may be balanced by the head without motion ($\mathbf{u}^{\langle 2\rangle} = 0$):

$$\Phi_a^{\langle 2\rangle} = -\frac{\rho_a a^4}{2r^2}, \quad \Phi^{\langle 2\rangle} = \frac{2a^4}{r^4}\hat{\beta} - \frac{\rho a^4}{2r^2} \tag{16), (17}$$

and

$$\Phi_w^{\langle 2\rangle} = -\rho_w a^4/2r^2. \tag{18}$$

The interface condition (4) is satisfied because $u^{\langle 2\rangle} = w^{\langle 2\rangle} = 0$. The interface condition (5) is satisfied identically because $S_{z\theta}$ and $S_{r\theta}$ are odd functions of Ω. The interface condition (6) at order two is satisfied identically when $\mathbf{u}^{\langle 2\rangle} = 0$. In the same way, it is easy to verify that interface terms arising from S_{nn} and D_{nn} vanish at second order when $\mathbf{u}^{\langle 2\rangle} = 0$.

Combining all these results we find that at second order (7) and (8) reduce to

$$-\frac{2a^4}{r^4}\hat{\beta} + (\rho - \rho_a)\frac{a^4}{2r^2} + (\rho - \rho_a) g h_T^{\langle 2\rangle} - \frac{T_T}{r}(r h_T'^{\langle 2\rangle})' = 0 \tag{19}$$

and

$$-\frac{2a^4}{r^4}\hat{\beta} + (\rho - \rho_w)\frac{a^4}{2r^2} + (\rho - \rho_w) g h_B^{\langle 2\rangle} + \frac{T_B}{r}(r h_B'^{\langle 2\rangle})' = 0. \tag{20}$$

Equations (19) and (20) are to be solved subject to the conditions

$$h_T'^{\langle 2\rangle}(a) = h_B'^{\langle 2\rangle}(a) = 0 \tag{21}$$

and

$$h_T'^{\langle 2\rangle}(r),\ h_B'^{\langle 2\rangle}(r) \to 0 \tag{22}$$

as $r \to \infty$. Equations (19) and (20) and the boundary conditions are decoupled. There is no interaction between the top and bottom at second order. Each boundary-value

problem is of the form of equation (15.2) of I or equation (4.16) of II and the approximations used there apply here. We find that the height rises at the rod may be approximated by

$$h_T^{\langle 2\rangle}(a) \sim \frac{a}{2T_T\sqrt{S_T}}\left[\frac{4\hat{\beta}}{4+\lambda_T} - \frac{(\rho-\rho_a)\,a^2}{2+\lambda_T}\right] \tag{23}$$

and

$$h_B^{\langle 2\rangle}(a) \sim \frac{-a}{2T_B\sqrt{S_B}}\left[\frac{4\hat{\beta}}{4+\lambda_B} + \frac{(\rho_w-\rho)\,a^2}{2+\lambda_B}\right], \tag{24}$$

where $$\lambda^2 = a^2S, \quad S_T = (\rho-\rho_a)\,g/T_T, \quad S_B = (\rho_w-\rho)\,g/T_B$$

and

$$h^{\langle 2\rangle} = [dh(r,\Omega)/d\Omega^2]_{\Omega=0}. \tag{25}$$

Equations (19) and (23) show that normal stresses elevate and inertia depresses the STP–air interface. At this interface there is a critical radius: for values of r smaller than this critical value normal stresses dominate; for larger values inertia dominates. Equations (20) and (24) show that normal stresses and inertia have the same sign and both depress the water–STP interface; a critical radius does not exist.

Equation (23) was used in I and II (with $\rho_a = 0$) to compute the value of the climbing constant from measurements of the height rise

$$h(a,\Omega) \sim h^{\langle 2\rangle}(a)\,\Omega^2. \tag{26}$$

In our experiments we floated STP (depth = 3·8 cm) on distilled water (depth = 6·0 cm) in a square container of side 29·2 cm. The surface tension of STP against air and the interfacial tension of STP and water were determined by standard procedures using a ring tensiometer. The values of the relevant physical parameters are

$$\rho-\rho_a = 0{\cdot}88\,\mathrm{g/cm^3}, \quad \rho_w-\rho = 0{\cdot}12\,\mathrm{g/cm^3}, \quad T_T = 31\,\mathrm{dynes/cm}, \quad T_B = 28\,\mathrm{dynes/cm}.$$

The viscosities of the three fluids differ by many orders of magnitude:

$$(\mu_a, \mu_w, \mu) \sim (0{\cdot}00018, 0{\cdot}011, 150)\,\mathrm{g/cm\,s}.$$

This implies that the STP may be regarded as free of viscous tractions induced by the motion of air and water at each interface. It is perhaps worth noting that the viscosity does not enter our analysis up to second order. It is therefore not necessary to approximate the continuity of stresses with stress-free boundary conditions even though such an approximation is justified in the present problem.

To test the theory of this paper we measured the height rise at $r = a$ from simultaneous photographs of the up-climb in air and the corresponding down-climb in water. These measurements are summarized in figures 2(*a*) and (*b*). It is apparent that there is a measurable interval of values of Ω^2 over which the rise is linear in Ω^2. For these values, (26) is supposed to hold simultaneously for both interfaces. The experimental values of $h_T^{\langle 2\rangle}(a)$ and $h_B^{\langle 2\rangle}(a)$ are then given by the slopes of the lines in figures 2(*a*) and (*b*).

Turning next to (23) and (24) we note that the values of all of the quantities except $\hat{\beta}$ are known. To be consistent with theory it is necessary that every measured value of the slope, for each rod, must yield one and the same value of $\hat{\beta}$. The values of $\hat{\beta}$ computed in this way are summarized in table 1. There is good agreement between the corresponding values of the climbing constant obtained from the STP–air interface and the STP–water interface. These values are also compared with values for $\hat{\beta}$

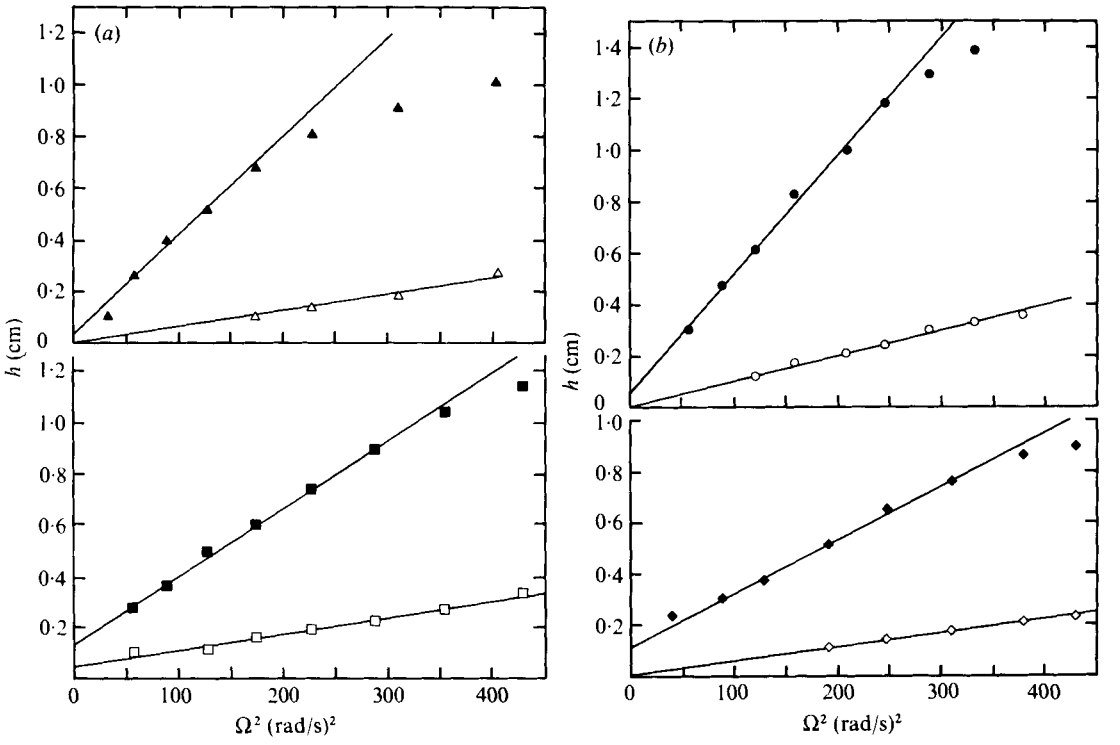

FIGURE 2. Measured values of the height rise at $r = a$. Open symbols, air; filled symbols, water. □, $a = 0{\cdot}479$ cm, temperature = 27·8 °C; △, $a = 0{\cdot}951$ cm, temperature = 27·8° C; ○, $a = 0{\cdot}627$ cm, temperature = 23·5 °C; ◇, $a = 0{\cdot}627$ cm, temperature = 28·2 °C.

computed from the temperature relationship given in II for a different sample of STP, namely

$$\hat{\beta} = 20\exp(-0{\cdot}115T)\,\mathrm{g/cm}. \tag{27}$$

The differences between the values of $\hat{\beta}$ measured in these experiments and the values predicted from (27) are comparable to the discrepancies between (27) and the values of some of the original data points used in establishing (27).

Figure 3 (plate 1) shows photographs of the up-climb and down-climb corresponding to four different values of Ω. For technical reasons we were unable to photograph the up-climb and down-climb on a single photograph using only one camera. Thus the photographs of the free surfaces on the bottom and top were taken simultaneously using two cameras. The photographs were taken at grazing incidence across the interfaces, and were then spliced together for presentation in figure 3. The resulting composite is an accurate representation of the situation more clearly seen in the sketch in figure 1. The reader is cautioned against confusing mirror reflexions in the free surface with the actual rise. The fluid rises at the upper free surface and sinks at the bottom free surface.

For a given frequency Ω and a given rod the ratio of the down-climb to the up-climb is given approximately by $h_B^{\langle 2\rangle}(a)/h_T^{\langle 2\rangle}(a)$ [see (23) and (24)]. It is usual that the term arising from inertia which is proportional to a^2 is neglible. Then

$$\frac{h_B^{\langle 2\rangle}(a)}{h_T^{\langle 2\rangle}(a)} \sim \frac{[T_T(\rho-\rho_a)]^{\frac{1}{2}}\{4+a[(\rho-\rho_a)g/T_T]^{\frac{1}{2}}\}}{[T_B(\rho_w-\rho)]^{\frac{1}{2}}\{4+a[(\rho_w-\rho)g/T_B]^{\frac{1}{2}}\}}.$$

Rod radius (cm)	Temperature (°C)	β Air/STP	β Water/STP	β (from II)
0·479	27·8	0·78	0·78	0·82
0·627	23·5	1·07	1·10	1·34
0·627	28·2	0·65	0·49	0·78
0·951	27·8	0·83	0·66	0·82

TABLE 1

Under the conditions prevailing in our experiment, this ratio is

$$\frac{h_B^{\langle 2\rangle}(a)}{h_T^{\langle 2\rangle}(a)} \sim \left(\frac{\rho-\rho_a}{\rho_w-\rho}\right)^{\frac{1}{2}} \left(\frac{1{\cdot}05+1{\cdot}48a(\rho-\rho_a)^{\frac{1}{2}}}{1+1{\cdot}48a(\rho_w-\rho)^{\frac{1}{2}}}\right). \tag{28}$$

A further approximation to this ratio for small values of a is

$$\frac{h_B^{\langle 2\rangle}(a)}{h_T^{\langle 2\rangle}(a)} \sim \left(\frac{\rho-\rho_a}{\rho_w-\rho}\right)^{\frac{1}{2}} \sim 2{\cdot}7.$$

For the rods used in our experiments, the values of the ratio computed from (28) are 3·7, 3·9 and 4·3 for $a = 0{\cdot}479$, 0·627 and 0·951 cm. Figures 2(a) and (b) show that these values are in good agreement with the measured values when Ω is small.

Larger amplification ratios may be achieved by floating the test fluid on Newtonian liquids of slightly greater density. A similar analysis may be constructed when the two bottom fluids are both viscoelastic.

2. Symmetry-breaking bifurcation of time-periodic flow induced by torsional oscillation of a rod (the 'flower' instability)

In a recent study (Joseph 1976*a*) a general theory of perturbations of the rest state of a simple fluid with an arbitrary time-dependent motion was presented. The theory was applied (Joseph 1976*b*) to the problem of the free surface induced by torsional oscillations $\mathbf{u} = \mathbf{e}_\theta a\epsilon \sin\omega t$ of a rod. When the amplitude ϵ of the oscillation ($\epsilon = \frac{1}{2}\omega\Theta$, where Θ is the *angle of twist*) is small the theory predicts a mean climb plus an oscillating climb of frequency 2ω. Both components of the climb are axisymmetric. Experiments by Beavers (1976) are in good agreement with the theory and show further that the oscillating part of the climb is barely visible to the naked eye. The mean climb is constant in time and is smaller in magnitude than in the case of steady rotation at a value of Ω equal to the root-mean-square value in unsteady flow. When ϵ is large the axisymmetric time-periodic motion loses its stability to what appears to be another time-periodic motion with the same period but with a different symmetry pattern. The new symmetry pattern has a certain number of petals which are determined by operating conditions. In figure 4 (plate 2) we display photographs of three- and four-petal configurations which bifurcate from time-periodic flow. The experiments for figure 4 were performed with TL-227 (Texaco Oil Co.), for which the normal stresses are roughly twenty times as great as those which develop in STP.

This work was supported by the U.S. Army Research Office.

REFERENCES

BEAVERS, G. S. 1976 *Arch. Rat. Mech. Anal.* **62**, 343.

BEAVERS, G. S. & JOSEPH, D. D. 1975 *J. Fluid Mech.* **69**, 475.

JOSEPH, D. D. 1976*a* *Stability of Fluid Motions* II, chap. 13. *Tracts in Natural Philosophy.* Springer.

JOSEPH, D. D. 1976*b* *Arch. Rat. Mech. Anal.* **62**, 323.

JOSEPH, D. D., BEAVERS, G. S. & FOSDICK, R. L. 1973 *Arch. Rat. Mech. Anal.* **49**, 381.

SAVILLE, D. A. & THOMPSON, D. W. 1969 *Nature* **223**, 391.

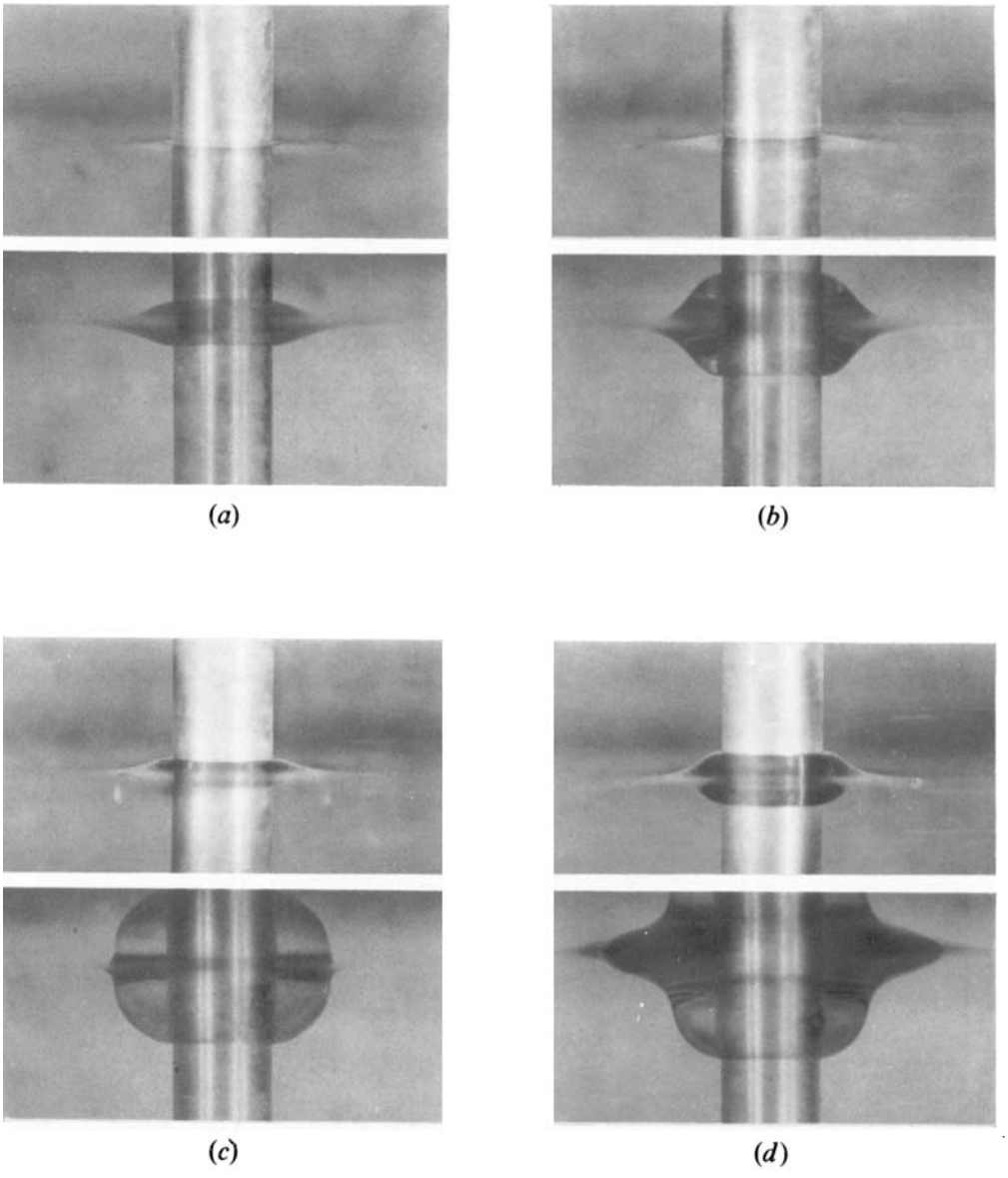

FIGURE 3. The free surfaces of STP floating on water (see figure 1). Rod radius = 0·627 cm. Angular velocity, Ω: (*a*) 7·5; (*b*) 11·0; (*c*) 14·5; (*d*) 19·5 rad/s. The STP climbs up into air and down into water. The reader is cautioned against confusing mirror reflexions in the free surface with the actual rise.

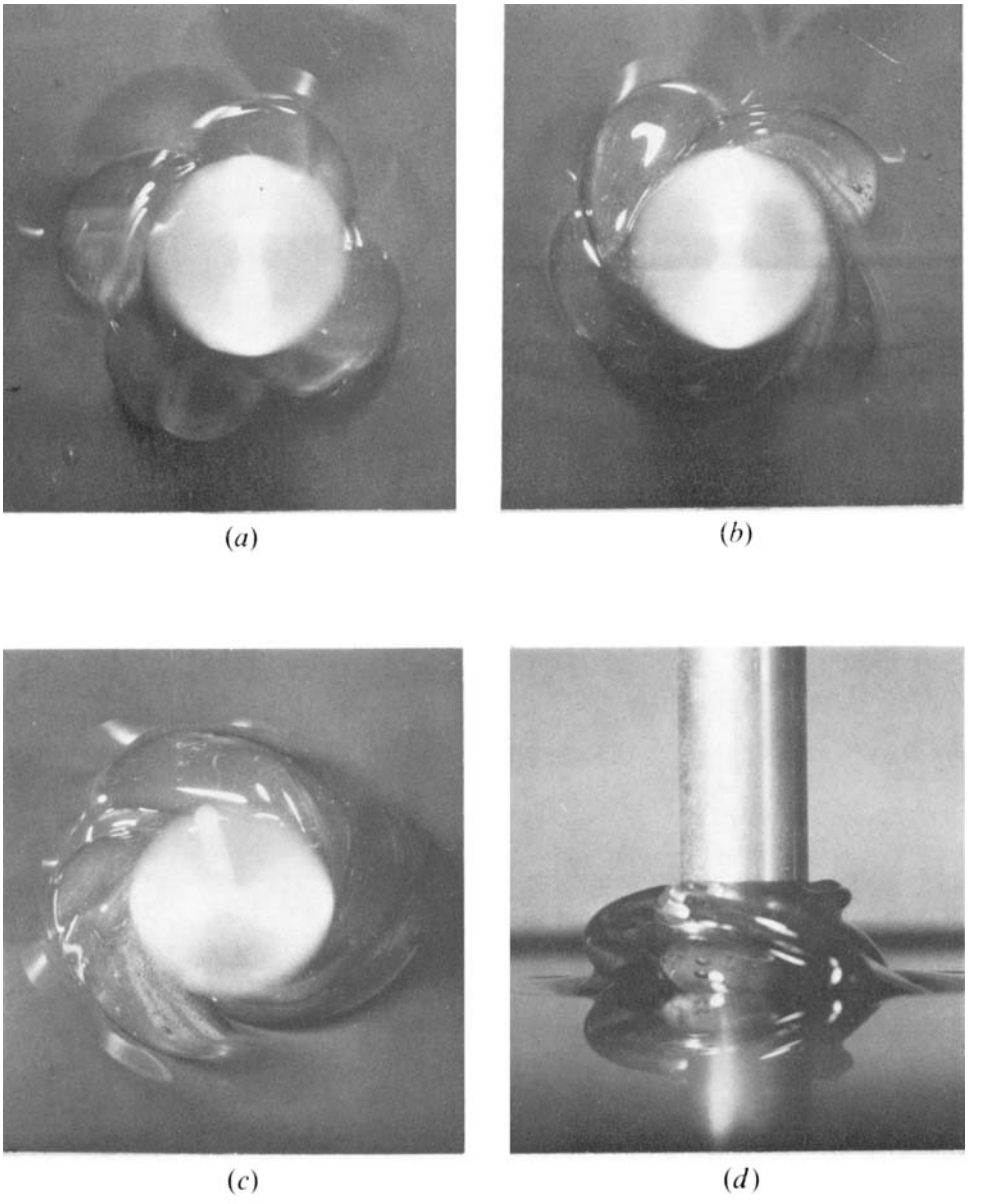

FIGURE 4. (*a*), (*b*) Top views of the four-petal configurations bifurcating from an axisymmetric time-periodic flow. The two views are photographs at two different instants during a cycle: $\omega = 9{\cdot}5$ cycles/s, $\Theta = 200°$. (*c*) Top view and (*d*) side view of the three-petal configuration bifurcating from an axisymmetric time-periodic flow: $\omega = 9{\cdot}2$ cycles/s, $\Theta = 235°$.